

# Dispersion in magnetostatic CoTaZr spin wave-guides

A. Kozhanov, D. Ouellette, Z. Griffith, M. Rodwell, S. J. Allen

California Nanosystems Institute, University of California at Santa Barbara, Santa Barbara, CA, 93106

A. P. Jacob

Technology and Manufacturing Group,

Intel Corporation, Santa Clara, CA 95052 & Western Institute of Nanoelectronics (WIN), UCLA, Los Angeles, CA 90095

D. W. Lee and S. X. Wang

Department of Materials Science and Engineering, Sanford University, Stanford, CA, 94305

(Received )

Magnetostatic spin wave dispersion and loss are measured in micron scale spin wave-guides in ferromagnetic, metallic CoTaZr. Results are in good agreement with model calculations of spin wave dispersion and up to three different modes are identified. Attenuation lengths of the order of  $3 \mu\text{m}$  are several of orders of magnitude shorter than that predicted from eddy currents in these thin wires. (PACS: 76.50.+g)

A current technology drive, directed toward future signal processing and logic devices, attempts to introduce spin degrees of freedom as an alternative, complement or companion to semiconductor charge based electronics. Magnetic bipolar transistors<sup>1</sup>, spin MOSFETs<sup>2,3</sup> and spin torque transfer devices<sup>4,5,6</sup> explore potential performance enhancement by sensing or using the spin degree of freedom that accompanies the charge current flow<sup>7</sup>. Spin waves can transfer spin information and have the potential for spin control without directly moving charge. For example, spin wave interference could be used in Mach-Zehnder type interferometer as a wave based logical element.<sup>8,9,10</sup> Further, spin waves are intrinsically non-linear<sup>11,12</sup>; interaction of the spin wave with a locally controlled magnetization could lead to a spin wave switch.

Microwave devices like delay lines, filters and resonators based on magneto-static waves in insulating ferrimagnetic materials like yttrium-iron garnet (YIG)<sup>13</sup> have long been explored and developed. However, future micro and nano scale spin wave logic devices may benefit from exploiting ferromagnetic metals that are more easily deposited, processed and nanofabricated than ferrimagnetic oxides. Further, ferromagnetic metals like CoTaZr and CoFe have nearly an order of magnitude larger saturation magnetization than typical ferrimagnets.<sup>14</sup> As a result, they will support higher, shape defined, zero magnetic field resonances and consequently intrinsically faster response. Configurations that support spin wave modes without requiring external magnetic fields are essential for future micro/nanodevices. Spin wave damping by eddy currents must be mitigated but dipolar magnetostatic waves are little affected by material discontinuity and micro and nanostructuring can diminish eddy current losses.

This letter describes excitation, detection and propagation of backward volume magnetostatic spin waves (BVMSW) in ferromagnetic wires.<sup>15</sup> The magnetization lies along the axis of the wire due to strong shape anisotropy. In the *absence* of a magnetic field, it has a finite ferromagnetic resonance determined by the cross sectional shape and supports backward volume spin waves propagating along the wire.

Co<sub>90</sub>Zr<sub>5</sub>Ta<sub>5</sub> ferromagnetic films, 110 nm thick, were grown by sputter deposition on a Si/SiO<sub>2</sub> substrate. A vibrating sample magnetometer measured a saturation magnetization of

$M_s \approx 1.2\text{T}$  and a coercive field of  $H_c \approx 2\text{Oe}$  in the unpatterned film. Wires were produced with a Panasonic ICP etch system using chlorine chemistry. An insulating SiO<sub>2</sub> layer covered the patterned ferromagnetic wires.

Magnetostatic spin waves were excited and detected by coupling loops formed by the short-circuited ends of coplanar waveguides<sup>16</sup>. (Figure 1.) High frequency currents in the signal line of the coplanar waveguide, aligned atop the ferromagnetic wire, produced magnetic fields that excite the magnetostatic spin waves as shown in Figure 2. Because of the high permeability of the CoTaZr perpendicular to the wire, the high frequency magnetic field is largely outside the wire.<sup>17,18,19</sup> This causes poor but sufficient coupling to excite and detect the magnetostatic waves.

S-parameters were measured at room temperature using an HP8510 and Agilent 8720ES vector network analyzers. Only S<sub>12</sub>, the ratio of high frequency voltage at terminals 1 to the input high frequency voltage at terminals 2 is analyzed in the following discussion. The test devices were positioned on the narrow gap of small electro-magnet that provided bias up to 1000 Oe. By comparing the S-parameters at disparate bias magnetic fields, the magnetic field independent instrument response can be effectively removed to expose the S-parameters of the magneto-static spin wave guide.

Figure 3 displays the real part of the magneto-static spin wave contribution to S<sub>12</sub>. A strong resonant feature moves to

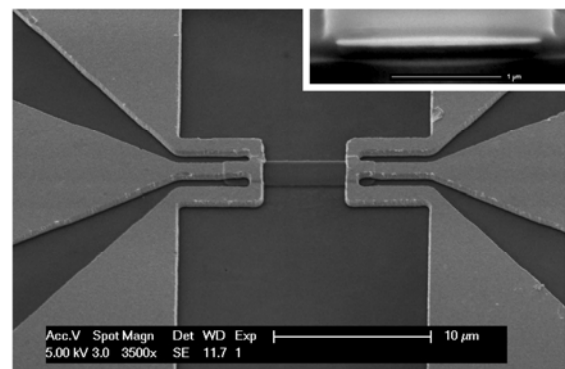


FIG.1. SEM image of a  $(10 \times 1.8 \times 0.11) \mu\text{m}^3$  CoTaZr spin wave-guide excited and detected by shorted coplanar waveguides. Inset: Cross section through spin wave guide.

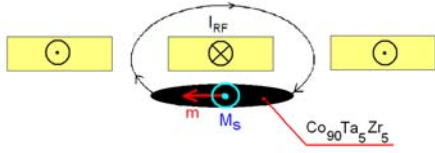


FIG 2. Schematic cross section through the coplanar waveguide above the ferromagnetic metallic wire.

high frequency with increasing magnetic field. At a particular magnetic field, there is very little signal at frequencies below the strong feature whereas at higher frequencies many discernible “noise like”, but reproducible, features appear. It should also be noted that the amplitude of the transmitted signal “turns on” with a modest magnetic field and then exhibits little growth with further magnetic bias. Micromagnetic simulations confirm that without a small bias field,  $\sim 50$  Oe, the magnetization, at the wire ends, under the coupling loops is not well aligned and the coupling to the spin excitations suppressed.

The real and imaginary parts of  $S_{12}$  for a  $(5 \times 1.8 \times 0.11) \mu\text{m}^3$   $\text{Co}_{90}\text{Zr}_5\text{Ta}_5$  wire with a bias of 594 Oe are shown in figure 4. Despite the large variations in the amplitude,  $|S_{12}|$ , a polar plot, figure 4b, shows the phase making a steady evolution as the frequency increases from 8 to 13 GHz. Despite the “noise like”

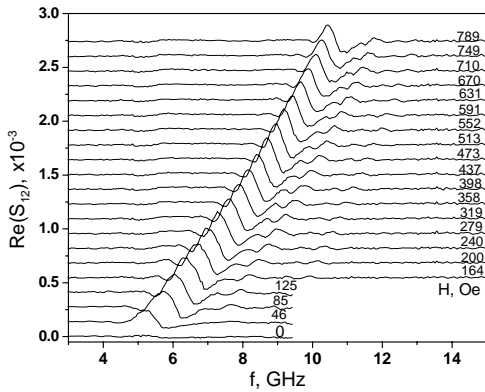


FIG 3. Frequency dependence of the real part of  $S_{12}$  for a  $5 \mu\text{m}$  long  $\text{CoZrTa}$  wire at different longitudinal bias magnetic fields.

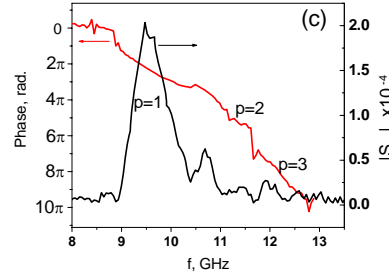
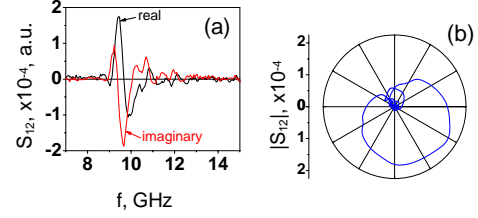
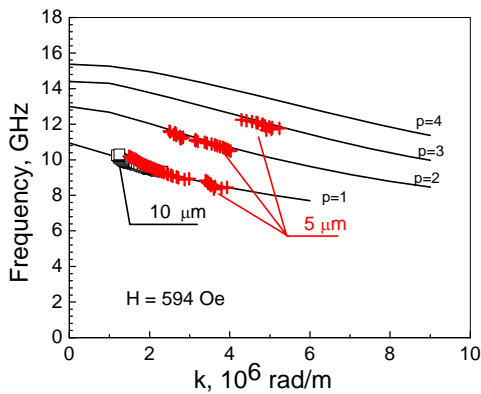


FIG 4. a) Frequency dependence of the real and imaginary parts of  $S_{12}$ , b) polar plot of  $S_{12}$  amplitude and phase, and c) Cartesian plot of  $S_{12}$  amplitude and phase, measured at  $H=594$  Oe on the structure with  $(5 \times 1.8 \times 0.11) \mu\text{m}^3$  a  $\text{CoTaZr}$  wire.

but *reproducible* amplitude spectrum, the phase appears to wind in a piecewise continuous fashion through  $10\pi$  radians. While the relative phase of  $S_{12}$  evolves smoothly when the amplitude is strong, near minima in  $S_{12}$  the phase appears to jump by  $\pi$  radians before continuing to wind in a well-defined manner as the transmitted signal grows again. A Cartesian plot of the same is shown in figure 4c.

The evolution of the phase of  $S_{12}$  suggests that spin waves couple the two coplanar waveguides. In particular, if we assume that the effective separation between the point of excitation and detection is  $r$  then the frequency dependent phase,  $\varphi(f)$ , can be simply related to a frequency dependent wave vector,  $k(f)$ , by  $\varphi(f) \approx k(f)r + \varphi_0$ .  $\varphi_0$  is an unknown, but assumed constant, phase and  $r$  is a length separating excitation and detection. We guide our interpretation by calculating the spin wave dispersion following Arias and Mills<sup>20,21</sup>.

As we invert the phase-frequency data we are compelled to

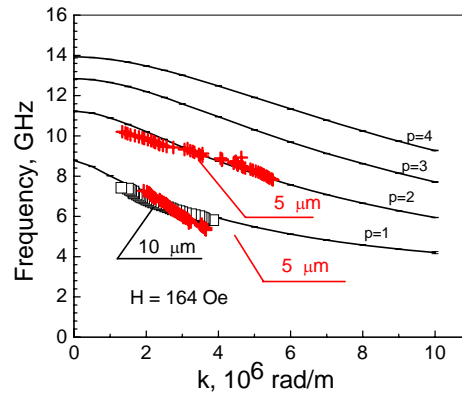


FIG 5. Measured dispersion for  $5 \mu\text{m}$  long (crosses) and  $10 \mu\text{m}$  long (squares)  $\text{CoTaZr}$  wires with  $(1.8 \times 0.11) \mu\text{m}^2$  elliptical profile at 594 Oe. Calculated dispersion (solid lines) for elliptical cross section wires<sup>20,21</sup>. Left: Bias field 594 Oe. Right: Bias field 164 Oe.

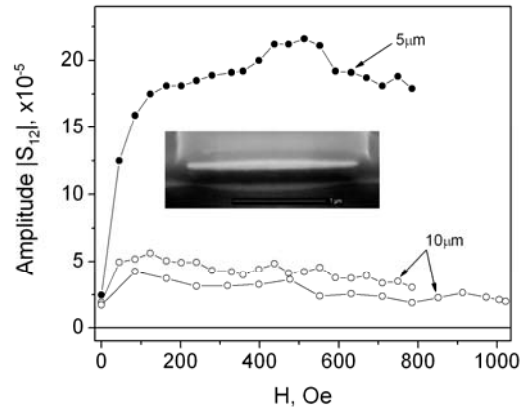


FIG. 6. Peak signal  $|S_{12}|$  vs magnetic field for 5 and 10  $\mu\text{m}$  CoTaZr wires with  $(1.8 \times 0.11) \mu\text{m}^2$  elliptical profile.

associate different frequency ranges with the different spin wave modes which, according to the model calculations, have different spatial distributions in the cross section of the wire. They are indexed by  $p=1, 2, 3 \dots$  following the notation of Arias and Mills. The phase vs frequency data is displayed in figure 5. as  $f_p(k)$  for the three lowest spin wave modes supported by the elliptical wire.

Note that figure 5. includes data from 5  $\mu\text{m}$  and 10  $\mu\text{m}$  long wires. The value of “ $r$ ” is only roughly known; we have simply taken the full length of the 5 and 10  $\mu\text{m}$  wires. *The simple scaling that brings the 10 and 5  $\mu\text{m}$  wires into reasonable agreement anchors our interpretation that the shorted coplanar waveguides are coupled by spin waves.*

The coupling to various spin waves should be determined by the Fourier components in the exciting field distribution. If the local excitation (and detection) has a spatial scale,  $\delta r$ , set by the exciting fields near the ends of the coplanar waveguides, we estimate that the strongest Fourier component occurs for spin wavelengths or wave vectors given by  $\delta r \sim \frac{\lambda}{2} = \frac{\pi}{k} \sim 1 \mu\text{m}$ .

This estimate compares favorably with the range of wavevectors of the modes identified in figure 5, approximately  $1-5 \cdot 10^6 \text{ m}^{-1}$ .

Figure 6. displays the amplitude of the peak transmitted signal versus magnetic field for both 5 and 10  $\mu\text{m}$  long wires. As noted and discussed earlier the signal grows quickly then remains relatively constant. Field attenuation lengths of  $l \sim 3 \mu\text{m}$  can be estimated by comparing the 10 and 5  $\mu\text{m}$  wires.

Following the model developed by Almeida and Mills<sup>22</sup> we estimate eddy current losses for our 110 nm thick film and find that they are 2-3 orders of magnitude *too small*, to account for the apparent decay length of  $\sim 3 \mu\text{m}$ . The ferromagnetic resonance linewidth for the unprocessed films is  $\sim 500 \text{ MHz}$ . Combined with the group velocity deduced from Figure 5 we estimate attenuation lengths by  $l \sim \left| \frac{d\omega}{dk} \right| \cdot \tau$  of order of  $\sim 1-2 \mu\text{m}$  and reasonably close to that deduced from Figure 6. It appears that the spin wave decay is caused by spin or magnetization relaxation rather than eddy current damping.

In summary, we have coupled high frequency coplanar waveguides by magneto-static spin waves in ferromagnetic CoTaZr metal wires; spin wave dispersion appears as a frequency and length dependent phase shift. Attenuation lengths

are approximately 3  $\mu\text{m}$ 's and much shorter than predicted by eddy current damping. Using the the Arias and Mills calculation of spinwave dispersion for infinitely long “wires”, we identify up to three different spin wave modes. Magnetic field bias dependence indicates that the spinwave excitation in these wires is sensitive to magnetization alignment and disorder.

These results indicate that spin wave interferometers fabricated with these materials will need to be of the order of or less than microns but magnetostatic spin waves can be “switched” or controlled by local magnetization.

This work is supported by NERC via the Nanoelectronics Research Initiative (NRI), by Intel Corp. and UC Discovery at the Western Institute of Nanoelectronics (WIN) Center.

<sup>1</sup> M. E. Flatté, Z. G. Yu, E. Johnston-Halperin and D. D. Awschalom, Appl. Phys. Lett., 82, 4740 (2003).

<sup>2</sup> S. Datta and B. Das, Appl. Phys. Lett., 56, 665 (1990).

<sup>3</sup> S. Sugahara and M. Tanaka, ACM Trans. Stor., 2, 197 (2006).

<sup>4</sup> I. J. C. Slonczewski, J. Magn. Magn. Mater. 159, L1 (1996).

<sup>5</sup> L. Berger, Phys. Rev. B 54, 9353 (1996).

<sup>6</sup> E. B. Myers, D. C. Ralph, J. A. Katine, R. N. Louie, R. A. Buhrman, Science 285, 867 (1999).

<sup>7</sup> I. Žutić, J. Fabian, S. Das Sarma, Rev. Mod. Phys. 76, 323 (2004).

<sup>8</sup> M. Bailleul, D. Olligs, C. Fermon, and S.O. Demokritov, Europhys. Lett., 56, 741 (2001).

<sup>9</sup> M. Bailleul, D. Olligs, and C. Fermon, Appl. Phys. Lett. 83, 972 (2003).

<sup>10</sup> M.P. Kostylev, A.A. Serga, T. Schneider, B. Leven, and B. Hillebrands, Appl. Phys. Lett. 87, 153501(2005).

<sup>11</sup> B. Kalinikos, N.G. Kovshikov, and C.E. Patton, Phys. Rev. Lett., 80, 4301 (1998).

<sup>12</sup> B.A. Kalinikos, N.G. Kovshikov and C.E. Patton, Appl. Phys. Lett. 75, 265 (1999).

<sup>13</sup> A review: J.D. Adam, L.E. Davis, G.F. Dionne, E.F. Schloemann and S.N. Stitzer, IEEE. Trans. Microwave Theory Tech. 50, 721 (2002).

<sup>14</sup> B.Kuanr, I.R. Harward, D.L. Marvin, T. Fal, R.E. Camley, D.L. Mills, and Z. Celinski, IEEE Trans. Magnetics, 41, 3538 (2005).

<sup>15</sup> Infinite thin ferromagnetic films support three different modes of propagation depending on the relative orientation of the magnetization, applied magnetic field and the wave vector,  $\vec{k}$  - surface waves (MSSW) when  $\vec{k} \perp \vec{M}$  ( $\vec{M}$  and  $\vec{H}$  in the plane), backward volume waves (MSBVW) when  $\vec{k} \parallel \vec{M}$  ( $\vec{M}$  and  $\vec{H}$  in the plane) and forward volume waves when  $\vec{k} \perp \vec{M}$  ( $\vec{M}$  and  $\vec{H}$  perpendicular to the plane). R.W. Damon and J.R. Eshbach, J.Chem. Phys. Solids, 19 308 (1961); R.W. Damon and H. van der Vaart, J. Appl. Phys., 36, 3453 (1965); J.D. Adam and J.H. Collins, Proc. IEEE, 64, 794 (1976).

<sup>16</sup> M.V. Costache, M. Sladkov, C.H. van der Wal, and B.J. Wees, Appl. Phys. Lett., 89, 192506 (2007).

<sup>17</sup> R.M. Fano, L.J. Chu and R.B. Adler, *Electromagnetic Fields, Energy and Forces* (John Wiley and Sons, Inc., 1960), p. 195-204.

<sup>18</sup> W.A. Roshen and D.E. Turcotte, IEEE Trans. Magnetics, 24, 3213 (1988).

<sup>19</sup> D.S. Gardner, G. Schrom, P. Hazucha, F. Paillet, T. Karnik, S. Borkar, J. Saulters, J. Owens and J. Wetzel, IEEE Trans. Magnetics, 43, 2615 (2007).

<sup>20</sup> R. Arias and D.L. Mills, Phys. Rev. B70, 094414(2004); R. Arias and D.L. Mills, Phys. Rev. B72, 104418 (2005)

<sup>21</sup> R.E. DeWames and T. Wolfram, Appl. Phys.Lett., 16, 305 (1970).

<sup>22</sup> N.S. Almeida and D.L. Mills, Phys. Rev. B, 53, 12232 (1996).